Narrowing the Search for Optimal Call-Admission Policies Via a Nonlinear Stochastic Knapsack Model

**Marco Cello · Giorgio Gnecco · Mario Marchese ·
Marcello Sanguineti**

Abstract Call admission control with two classes of users is investigated via a nonlinear stochastic knapsack model. The feasibility region represents the subset of the call space, where given constraints on the quality of service have to be satisfied. Admissible strategies are searched for within the class of coordinate-convex policies. Structural properties that the optimal policies belonging to such a class have to satisfy are derived. They are exploited to narrow the search for the optimal solution to the nonlinear stochastic knapsack problem that models call admission control. To illustrate the role played by these properties, the numbers of coordinate-convex policies by which they are satisfied are estimated. A graph-based algorithm to generate all such policies is presented.

M. Cello · M. Marchese
Department of Telecommunications, Electronic, Electric, and Naval Engineering (DITEN),
University of Genoa, Via Opera Pia, 11-16145 Genova, Italy
e-mail: marco.cello@unige.it

M. Marchese
e-mail: mario.marchese@unige.it

G. Gnecco
Institute for Advanced Studies (IMT), Piazza S. Ponziano, 6-55100 Lucca, Italy
e-mail: giorgio.gnecco@imtlucca.it; giorgio.gnecco@unige.it

G. Gnecco · M. Sanguineti (✉)
Department of Computer Science, Bioengineering, Robotics, and Systems Engineering (DIBRIS),
University of Genoa, Via Opera Pia, 13-16145 Genova, Italy
e-mail: marcello.sanguineti@unige.it

Mathematics Subject Classification (2000)   90B15 · 90B18 · 90C10 · 90C27 · 68M10

1 Introduction

Call admission control (*CAC*) aims at regulating the traffic volume in networks by determining when to accept or reject a new connection, flow, or call request. It is typically used in voice communications, particularly in wireless mobile networks and voice over internet protocol (VoIP). It can be exploited to guarantee specific *quality of service* (*QoS*) requirements on the load entering the network. The load is limited by verifying if enough resources are available to satisfy the performance requirements of an incoming call, without penalizing the calls already processed. The performances are measured, e.g., in terms of packet loss, delay, jitter, etc., and they are optimized by maximizing an objective represented, e.g., by the expected revenue associated with the accepted calls.

A useful combinatorial optimization model for CAC is represented by the knapsack problem. In the classical *deterministic knapsack*, a knapsack of a certain capacity is given, together with K classes of objects. Each object of class k has a fixed size b_k and generates a positive reward r_k. The objects can be placed into the knapsack as long as the sum of their sizes does not exceed the capacity. This represents a constraint that is linear in the decision variables, which correspond to the numbers n_k of chosen objects of each class k (see the inequality (1) in Sect. 2). The problem consists in placing the objects inside the knapsack so as to maximize the total reward.

In CAC for telecommunication networks, the objects are requests of connections coming from K different classes of users. Each user k is characterized by a bandwidth requirement b_k, which plays the role of the object size, and a duration. As the requests of connections from each of the K classes arrive randomly, and the durations of the connections are random, too, a stochastic extension of the knapsack is required to model CAC. It is called the *stochastic knapsack problem* in [1]. Among various possible such extensions (see, e.g., [2,3] and [4, Chapter 14]), we adopt the one proposed in [1], described as follows. The objects belonging to each class arrive according to exponentially distributed inter-arrival times, with means depending on the class and on the *state of the system*, represented by the number of objects of any class currently inside the knapsack. Every object has a sojourn time independent from the sojourn times of the other objects and described by a class-dependent distribution. An object from class k, if put into the knapsack, generates a revenue at a positive rate r_k. So, given a set of admissible policies, the problem consists in finding a policy that maximizes the average revenue (*optimal policy*), by accepting or rejecting the arriving requests of connections as a function of the current state. The linear constraint on the bandwidth defines a subset of the call space, where given QoS constraints are satisfied. Such a subset is called *feasibility region*.

Typically, in telecommunication networks a constraint linear in the decision variables n_k (see (1) in Sect. 2) arises when the bandwidth requirements b_k are characterized via their *peak rates* or *effective bandwidths*. Effective bandwidth [5] is a well-known concept, which aims at quantifying the amount of resources (between the

mean rate and the peak rate) for each connection, which, given an expected QoS, should be reserved in a multiplexing system, where many data streams share a common outgoing link. There exist various important contexts in which the linear constraint has to be replaced by a nonlinear one. For example, in statistical multiplexing with *dynamic service separation* (see, e.g., [6,7]), only cell streams from the same service (class of users) are allowed to be statistically multiplexed in a separate mini-buffer. The QoS provision for each mini-buffer (i.e., the cell-loss rate) can be supported by a weighted round robin. The scheduling weight of mini-buffer k is made directly proportional to a nonlinear function of n_k [8], which represents the minimum amount of link capacity required in order to meet the packet-level QoS requirements, when n_k connections are being served at the k-th mini-buffer. It is well known that, to reflect the economies of scale in statistically multiplexing cell streams, usually such a function of n_k increases monotonically with decreasing slope as n_k increases (see, e.g., [8,9]). Therefore, in general one has a nonlinearly constrained feasibility region. The corresponding model is referred to as *generalized stochastic knapsack problem*[1] (*GSK problem*) [10].

In general, finding optimal policies for both the stochastic knapsack [6, Chapter 4] and the GSK [11,12] problems is a difficult nonlinear combinatorial optimization task. The knowledge of structural properties of the optimal policies is useful to simplify its solution, or, at least, to find good suboptimal policies. For instance, for two classes of users, a feasibility region of the form (3) and an objective given by a weighted sum of per-class average revenues, structural properties were derived in [1] for the optimal policies belonging to the class of *coordinate-convex policies* (*CC policies*; see Sect. 2 for their definition). Such properties restrict the call state $(n_1, \ldots, n_K)$ of the CAC system to suitable subsets of the feasibility region. CC policies represent a large class of CAC policies. They are characterized by a relatively simple structure and interesting features, such as their associated product-form steady-state distribution [6, Chapter 4] and bounds on the per-class blocking probabilities [13]. Extensions to nonlinearly constrained feasibility regions of some structural results proved in [1] for linearly constrained ones were derived in [11,14]. Other structural results were obtained in [12].

The contributions of this paper are the following. For the GSK problem modeling CAC with two classes of users, we obtain closed-form expressions for the cardinalities of the sets of CC policies that satisfy various necessary optimality conditions derived in [11,12,14]. The results are useful to establish for which feasibility regions, such necessary optimality conditions restrict significantly the cardinalities of the sets of the associated *candidate optimal CC policies* with respect to the one of the set of all CC subsets of the regions themselves.

The paper is organized as follows. In Sect. 2, we describe the GSK model that we adopt to study CAC and investigate its properties. In Sect. 3, we summarize the structural properties obtained in [11,12,14] for the optimal CC policies. In Sect. 4, we investigate the numbers of CC policies satisfying some or all such properties. In Sect. 5, we provide an algorithm for the generation of such policies, together with some extensions of the obtained results. Sect. 6 contains a conclusive discussion.

---

[1] This is different from the generalized stochastic knapsack problem considered in [6, Chapter 3].

2 A Generalized Stochastic Knapsack for Call Admission Control: Model Statement and Properties

We start this section by stating the knapsack model used in the paper. In the classical *deterministic knapsack*, a knapsack of capacity $C > 0$ is given, together with K classes of objects. Each object of class $k \in \mathcal{K} := \{1, \dots, K\}$ has a fixed size $b_k > 0$ and generates a positive reward r_k. The objects can be placed into the knapsack as long as the sum of their sizes does not exceed C. This represents a constraint that is linear in the decision variables $n_k \geq 0$ (i.e., the number of objects of class k that are currently inside the knapsack):

$$\sum_{k \in \mathcal{K}} n_k b_k \leq C. \tag{1}$$

The problem consists in placing the objects into the knapsack in such a way as to maximize the total reward.

In general, in CAC one has a nonlinear constraint

$$\sum_{k \in \mathcal{K}} \beta_k(n_k) \leq C, \tag{2}$$

where the function $\beta_k(n_k)$ represents the minimum amount of link capacity needed in order to meet the packet-level QoS requirements, when n_k connections are being served at the k-th mini-buffer. As mentioned in Sect. 1, to reflect the economies of scale in statistically multiplexing cell streams, usually such a function increases monotonically with decreasing slope as n_k increases. The corresponding knapsack model, in which the linear constraint (1) is replaced by (2), is referred to as *generalized stochastic knapsack problem* (*GSK problem*) (see, e.g., [10]). In the context of admission control, the sets

$$\Omega_{FR} := \left\{ (n_1, \dots, n_K) \in \mathbb{N}_0^K : \sum_{k \in \mathcal{K}} n_k b_k \leq C \right\} \tag{3}$$

(in the linear case) and

$$\Omega_{FR} := \left\{ (n_1, \dots, n_K) \in \mathbb{N}_0^K : \sum_{k \in \mathcal{K}} \beta_k(n_k) \leq C \right\} \tag{4}$$

(in the nonlinear case) are called *feasibility regions*. They represent subsets of the call space $\{(n_1, \dots, n_K) \in \mathbb{N}_0^K\}$ where given QoS constraints are satisfied. Of course, the definition of feasibility region extends to sets satisfying other kinds of nonlinear constraints on the state space. As mentioned in Sect. 1, often linearly constrained feasibility regions arise as a consequence of the linearization of nonlinear QoS constraints (such a linearization is obtained by introducing the concept of "effective bandwidth"). Hence, considering the case of nonlinearly constrained feasibility regions appears to be quite well motivated, as usually the original constraints are themselves nonlinear.

The specific GSK model that we adopt for the CAC problem was first proposed in [1] for linearly constrained feasibility regions (stochastic knapsack) and extended in [11,12] to nonlinearly constrained ones (GSK). It is described as follows. The state of the CAC system with $K = 2$ classes of users is described by a 2-dimensional vector **n**, whose component n_k, $k = 1, 2$, represents the number of connections from users of class k that have been accepted by the system and are currently in progress. For each class k, the inter-arrival times are exponentially distributed with mean value $1/\lambda_k(n_k)$. The holding times of accepted connections are independent and identically distributed (i.i.d.) with mean value $1/\mu_k$. The CAC system accepts or rejects a request of connection according to a *coordinate-convex (CC) policy*. Here we recall its definition, from [6, p. 116].

Definition 2.1 A nonempty set $\Omega \subseteq \Omega_{FR} \subset \mathbb{N}_0^2$ is called coordinate-convex (CC) if and only if it has the following property: for each $\boldsymbol{n} \in \Omega$ with $n_k > 0$ one has $\boldsymbol{n} - \boldsymbol{e}_k \in \Omega$, where $\boldsymbol{e}_k$ is a 2-dimensional vector whose k-th component is 1, and the other one is 0. The CC policy associated with a CC set Ω admits an arriving request of connection if and only, if after admittance, the state process remains in Ω.

As there is a one-to-one correspondence between CC sets and CC policies, from now on we use the symbol Ω to denote both a CC set and the corresponding CC policy. From a geometric viewpoint, the meaning of a CC policy is that it always keeps the state vector inside a specific subset Ω of the state space and accepts an incoming request of connection if and only if, in case the request is granted, the state vector remains in Ω (this is not the case, e.g., of the so-called *trunk-reservation policies* [7]). Moreover, when a resource is released, the state vector remains inside Ω. One reason for which coordinate-convexity is used in CAC is the product-form steady-state distribution associated with CC policies (see formula (7)). We refer the reader to [15] for other variations of the concept of convexity.

Likewise in [11,12], in our analysis we consider the general case of a feasibility region Ω_{FR} characterized by a nonlinear constraint, described by a nonlinear upper boundary $(\partial\Omega_{FR})^+$ (see Fig. 1(b)). Similarly, we denote by $(\partial\Omega)^+$ the (linear or nonlinear) upper boundary of the CC set Ω. The set Ω_{FR} is assumed to be CC, as it often happens for feasibility regions defined in terms of QoS constraints (see, e.g., [16, Proposition 6.3]). Of course, this includes the particular case (3), which corresponds to a linear constraint.

Next proposition provides a characterization of CC sets. We let

$$l_2^\Omega(n_1) := \max\{j_2 \in \mathbb{N}_0 \text{ such that } (n_1, j_2) \in \Omega\} \, l_1^\Omega(n_2)$$
$$:= \max\{j_1 \in \mathbb{N}_0 \text{ such that } (j_1, n_2) \in \Omega\}. \tag{5}$$

The values $l_1^\Omega(n_2)$ and $l_2^\Omega(n_1)$ are the maximum numbers of type-1 and type-2 connections allowed in Ω when we have already n_2 type-2 / n_1 type-1 connections, respectively. It follows from the definitions that the functions $l_i^\Omega(\cdot)$ are nonincreasing. Set $n_{1,\max}^{\Omega_{FR}} := l_1^{\Omega_{FR}}(0)$ and $n_{2,\max}^{\Omega_{FR}} := l_2^{\Omega_{FR}}(0)$.
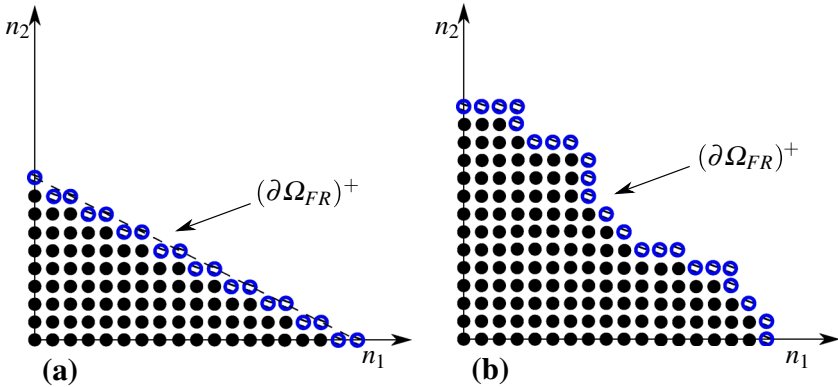
Fig. 1 The upper boundary $(\partial \Omega_{FR})^+$ of a feasibility region Ω_{FR} with 2 class of users for the case of **a** a linearly constrained Ω_{FR} (stochastic knapsack) and **b** a nonlinearly constrained Ω_{FR} (generalized stochastic knapsack, GSK)

Proposition 2.1 *The following two statements are equivalent.*

(i) Ω *is CC.*
(ii) *For $k = 1, 2$ and $t_k = 0, \ldots, n_{k,\max}^{\Omega_{FR}}$, consider the (one-dimensional) intersection I_{t_k} between Ω and the line of equation $n_k = t_k$. Denote by $\hat{k}$ the other index (i.e., if $k = 1$ then $\hat{k} = 2$, and if $k = 2$ then $\hat{k} = 1$). Only one of the three following cases can happen (see Fig. 2):*
(a) $I_{t_k} = \emptyset$;
(b) $I_{t_k} = \{0, \ldots, l_{\hat{k}}^{\Omega_{FR}}(t_k)\}$;
(c) *there exists an integer $n_{\hat{k}}(t_k) \in [0, l_{\hat{k}}^{\Omega_{FR}}(t_k))$ such that $I_{t_k} = \{0, \ldots, n_{\hat{k}}(t_k)\}$.*

Proof (i $\Rightarrow$ ii) Let us consider the case $k = 1$ (the proof for $k = 2$ is similar). If the set I_{t_1} is nonempty, then let (t_1, p_2) be such that $p_2 \in I_{t_1}$. An upper bound on the maximum possible value of p_2 is obviously $l_2^{\Omega_{FR}}(t_1)$, otherwise (t_1, p_2) would be outside Ω_{FR} and, since $\Omega \subseteq \Omega_{FR}$, it would be outside Ω, too.

By the coordinate-convexity of Ω, if $p_2 > 0$ then one has $(t_1, p_2 - 1) \in \Omega$, so $p_2 - 1 \in I_{t_1}$. Thus, by backward induction on p_2, only the three cases described in item (ii) are possible.

(ii $\Rightarrow$ i) Let $\boldsymbol{n} \in \Omega$ be such that at least one of its coordinates is greater than 0; suppose that such a coordinate is n_1. Then $n_1 \in I_{t_2}$ with $t_2 = n_2$. So, either the case (iib) or (iic) shows up. Then $n_1 - 1 \in I_{t_2}$, or, equivalently, $(n_1 - 1, n_2) \in \Omega$. Hence, Ω is CC. □

The objective to be maximized by the CAC system in the space $\mathcal{S}_{CC}(\Omega_{FR})$ of all CC subsets of Ω_{FR} (i.e., of all CC policies) is given by

$$J(\Omega) := \sum_{\boldsymbol{n} \in \Omega} (\boldsymbol{n} \cdot \mathbf{r}) P_{\Omega}(\boldsymbol{n}), \qquad (6)$$

Fig. 2 An example of the three cases described in Proposition 2.1 (ii)
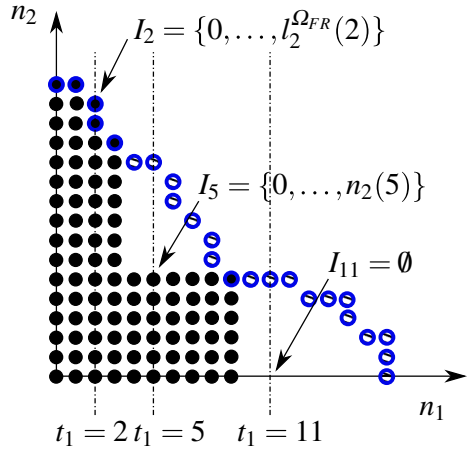
where **r** is a 2-dimensional vector, whose component r_k represents the instantaneous positive revenue generated by any accepted connection of class k that is still in progress, and $P_\Omega(\boldsymbol{n})$ is the steady-state probability that the CAC system is in the state $\boldsymbol{n}$. As Ω is CC, it is well known (see, e.g., [1]) that $P_\Omega(\boldsymbol{n})$ takes on the product-form expression

$$P_\Omega(\boldsymbol{n}) = \frac{\prod_{i=1}^{2} q_i(n_i)}{\sum_{\mathbf{m}\in\Omega} \prod_{i=1}^{2} q_i(m_i)}, \tag{7}$$

where

$$q_i(n_i) := \frac{\prod_{j=0}^{n_i-1} \lambda_i(j)}{n_i! \mu_i^{n_i}}. \tag{8}$$

Due to formulas (7) and (8), the objective (6) has quite a complicated expression. In particular, given any two CC sets $\Omega_1, \Omega_2 \subseteq \Omega_{FR}$, in general the relationship $\Omega_1 \subseteq \Omega_2$ does not imply $J(\Omega_1) \leq J(\Omega_2)$.

Next Proposition 2.2 (see also [17] for a similar approach) states that, in the case of homogeneous Poisson arrivals with rate λ_k for each class k, maximizing the objective (6) over the set of CC policies $\Omega \subseteq \Omega_{FR}$ is equivalent to minimizing the objective

$$J'(\Omega) := \sum_{k=1}^{2} \frac{\lambda_k}{\sum_{j=1}^{2} \lambda_j} \cdot \beta_k(\Omega) \tag{9}$$

over the same set, where $\beta_k(\Omega)$ is the blocking probability for the class k (i.e., the probability that an incoming connection request from class k is refused by the CC policy Ω). So, the objective $J'(\Omega)$ is a weighted sum of per-class blocking probabilities. The action of minimizing $J'(\Omega)$ is called *Erlang scheme* (see, e.g., [18]).

Proposition 2.2 *For $k = 1, 2$, let the arrivals from class k be homogeneous Poisson with rate λ_k. Set $r_1 := \frac{\mu_1}{\sum_{j=1}^{2} \lambda_j}$ and $r_2 := \frac{\mu_2}{\sum_{j=1}^{2} \lambda_j}$. Then $\mathrm{argmax}_{\Omega \in \mathcal{S}_{CC}(\Omega_{FR})} J(\Omega) = \mathrm{argmin}_{\Omega \in \mathcal{S}_{CC}(\Omega_{FR})} J'(\Omega)$.*

Proof Set $\bar{n}_k :=$ average number of class k users, $r_k :=$ revenue per unit time generated by a class k object, and $r_k \bar{n}_k :=$ average revenue per unit time generated by class k users. Then

$$J(\Omega) = \sum_{\boldsymbol{n} \in \Omega} \sum_{k=1}^{2} n_k r_k \, P_\Omega(n) = \sum_{k=1}^{2} r_k \sum_{n \in \Omega} n_k P_\Omega(\boldsymbol{n}) = \sum_{k=1}^{2} r_k \bar{n}_k. \qquad (10)$$

Let $L_k :=$ throughput of class k and $\frac{1}{\mu_k} :=$ mean service time for the objects of the class k. By Little's theorem [19] we get $\bar{n}_k = L_k \frac{1}{\mu_k}$, and (10) gives $J(\Omega) = \sum_{k=1}^{2} r_k L_k \frac{1}{\mu_k}$. So, in general, $J(\Omega)$ is a weighted sum (with weights r_k/μ_k) of the throughputs associated with the 2 classes.

As the arrivals for each class are homogeneous Poisson, it follows from [6, p. 20] that the relationship $L_k = \lambda_k(1 - \beta_k(\Omega))$ between throughput and blocking probability holds. Hence,

$$\sum_{k=1}^{2} r_k \frac{1}{\mu_k} L_k = \sum_{k=1}^{2} r_k \frac{1}{\mu_k} \lambda_k (1 - \beta_k(\Omega)) = \sum_{k=1}^{2} r_k \rho_k - \sum_{k=1}^{2} r_k \rho_k \beta_k(\Omega). \quad (11)$$

Finally, setting $r_1 := \frac{\mu_1}{\sum_{j=1}^{2} \lambda_j}$ and $r_2 := \frac{\mu_2}{\sum_{j=1}^{2} \lambda_j}$, we get

$$\mathrm{argmax}_{\Omega \in \mathscr{S}_{CC}(\Omega_{FR})} J(\Omega) = \mathrm{argmax}_{\Omega \in \mathscr{S}_{CC}(\Omega_{FR})} \left(\sum_{k=1}^{2} r_k \rho_k - \sum_{k=1}^{2} r_k \rho_k \beta_k(\Omega) \right)$$

$$= \mathrm{argmin}_{\Omega \in \mathscr{S}_{CC}(\Omega_{FR})} \sum_{k=1}^{2} r_k \rho_k \beta_k(\Omega) = \mathrm{argmin}_{\Omega \in \mathscr{S}_{CC}(\Omega_{FR})} J'(\Omega).$$

$\square$

Thanks to Proposition 2.2, from now on we can consider only the objective (6).

Next proposition investigates the robustness of an optimal CC policy with respect to changes in the feasibility region, all other parameters ($\lambda_k(\cdot)$, μ_k, r_k) being unchanged (see Fig. 3 for an interpretation of the result).

Proposition 2.3 *Let $\Omega^o \subseteq \Omega_{FR}$ be optimal for Ω_{FR}. Then, for every Ω'_{FR} such that $\Omega^o \subseteq \Omega'_{FR} \subseteq \Omega_{FR}$, Ω^o is optimal for Ω'_{FR}.*

Proof As $\mathcal{S}_{CC}(\Omega'_{FR}) \subseteq \mathcal{S}_{CC}(\Omega_{FR})$, we have $\min_{\Omega \in \mathcal{S}_{CC}(\Omega'_{FR})} J(\Omega) \geq \min_{\Omega \in \mathcal{S}_{CC}(\Omega_{FR})} J(\Omega)$. On the other hand, $\min_{\Omega \in \mathcal{S}_{CC}(\Omega_{FR})} J(\Omega) = J(\Omega^o) \geq \min_{\Omega \in \mathcal{S}_{CC}(\Omega'_{FR})} J(\Omega)$. $\square$
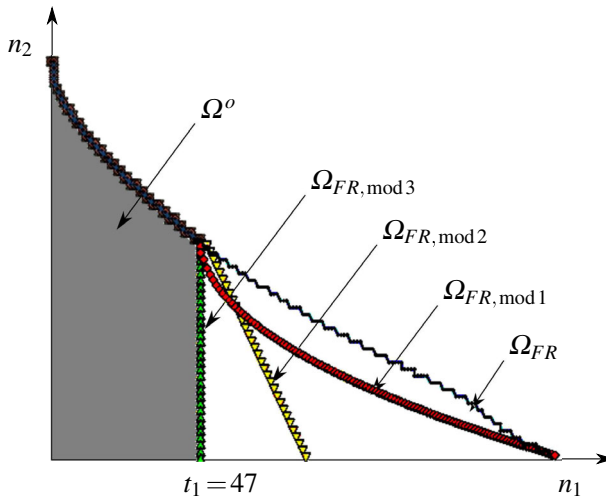
Fig. 3 The original feasibility region Ω_{FR} and three modified feasibility regions $\Omega_{FR,\,mod\,1}, \Omega_{FR,\,mod\,2}$, and $\Omega_{FR,\,mod\,3}$, obtained by removing states that do not belong to the CC set associated with an optimal CC policy Ω^o

3 Structural Properties of Optimal CC Policies

In this section, we recall some structural properties derived in [11,12,14] for the CC policies that maximize the objective (6) in the presence of nonlinearly constrained feasibility regions. In Sect. 4, we shall estimate the number of all the CC policies that satisfy some or all such properties.

Next Definition 3.1 is from [1].

Definition 3.1 The tuple $(\alpha, \beta) \in \Omega_{FR} \setminus \Omega$ is a type-1 corner point for Ω if and only if $\beta \geq 1$, $(\alpha, \beta - 1) \in \Omega$, and either $\alpha = 0$ or $(\alpha - 1, \beta) \in \Omega$; the tuple $(\alpha, \beta) \in \Omega_{FR} \setminus \Omega$ is a type-2 corner point for Ω if and only if $\alpha \geq 1$, $(\alpha - 1, \beta) \in \Omega$, and either $\beta = 0$ or $(\alpha, \beta - 1) \in \Omega$.

In the following, sometimes we shall use the term "corner point" to refer to either a type-1 or a type-2 corner point[2]. The importance of corner points emerges from next proposition from [14], according to which, in order to identify a CC policy (in particular, to find an optimal one), it is sufficient to consider its set of corner points. The proposition provides also a way to build a CC policy starting from the knowledge of merely its corner points.

Proposition 3.1 ([14]) *Let* $I(\Omega)$ *denote the set of corner points* $\{(\alpha_i, \beta_i)\}$ *of a CC set* $\Omega \subseteq \Omega_{FR}$, $|I(\Omega)|$ *its cardinality, and* $C_i^- := \{\mathbf{n} \in \Omega_{FR} : n_1 \geq \alpha_i \text{ and } n_2 \geq \beta_i\}$. *Then* $\Omega = (\Omega_{FR} \setminus \cup_{i=1}^{|I(\Omega)|} C_i^-)$.

---

[2] The notation used here is slightly different from the one of [1], where a distinction among "type-1 corner points," "type-2 corner points," and "corner points" is made.
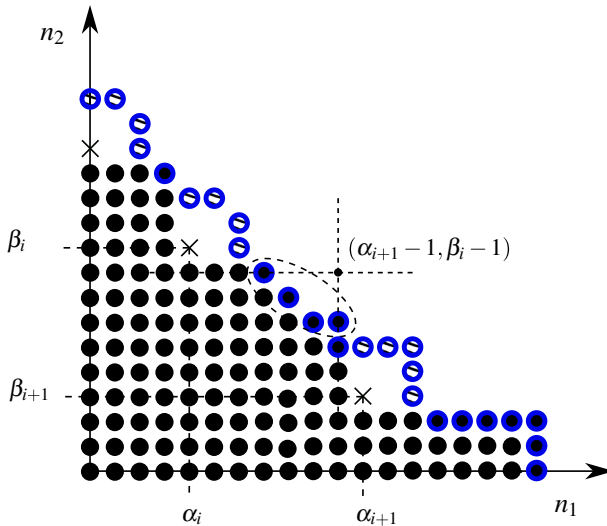
Fig. 4 Characterization of an optimal CC policy with at least 2 corner points, according to Theorem 3.2

Let Ω^o denote any optimal CC policy (or its associated CC set). Next result from [12] provides a characterization of the upper boundary $(\partial\Omega^o)^+$ of Ω^o and its intersection with $(\partial\Omega_{FR})^+$, when Ω^o has at least two corner points. Proposition 3.2 implies that between any two successive corner points the intersection between $(\partial\Omega^o)^+$ and $(\partial\Omega_{FR})^+$ is nonempty (see the dotted ellipse in Fig. 4). Proposition 3.3 complements Proposition 3.2, as it holds also for the case of a CC policy without corner points.

Proposition 3.2 ([12]) *Let (α_i, β_i) and $(\alpha_{i+1}, \beta_{i+1})$ be two consecutive corner points of Ω^o. Then the intersection between the vertical line $n_1 = \alpha_{i+1} - 1$ and the horizontal line $n_2 = \beta_i - 1$ either lies on $(\partial\Omega_{FR})^+$ or is outside Ω_{FR}.*

Proposition 3.3 ([14]) *Ω^o has a nonempty intersection with the upper boundary $(\partial\Omega_{FR})^+$ of Ω_{FR}.*

Next proposition from [11] extends to nonlinearly constrained feasibility regions a similar property derived in [1, Theorem 1] for linearly constrained ones. It states that the corner points of Ω^o can be located only among the points of a suitable grid (see Fig. 5)[3].

Proposition 3.4 ([11])

(i) If (α, β) is a type-2 corner point for Ω^o, then for some $j = 1, \ldots, n_{2,\max}^{\Omega_{FR}}$ one has

$$\alpha = l_1^{\Omega_{FR}}(j) + 1 \,. \tag{12}$$

---

[3] Not every combination of points in the grid is a feasible choice as a corner points. Indeed, by Definition 3.1 and the coordinate-convexity of Ω, no two corner points can be on the same vertical or horizontal lines.
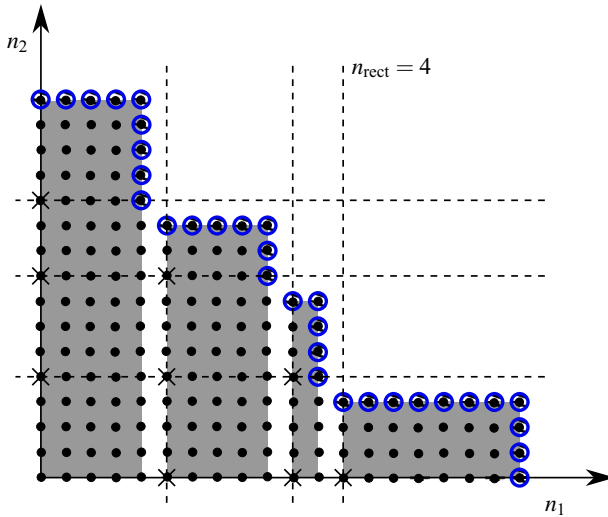
Fig. 5 Decomposition of the feasibility region into disjoint rectangles. The crosses represent the potential locations of corner points of an optimal CC policy, according to Proposition 3.4. Such locations define the grid G

(ii) If (α, β) is a type-1 corner point for Ω^o, then for some $j = 1, \ldots, n_{1,\max}^{\Omega_{FR}}$ one has

$$\beta = l_2^{\Omega_{FR}}(j) + 1. \tag{13}$$

The meaning of Proposition 3.4 is illustrated in Fig. 5. The result implies that the feasibility region can be decomposed as the union of a finite number n_{rect} of disjoint discrete rectangles with decreasing heights.

We define the grid G as the set of potential corner points whose coordinates satisfy (12) and (13). In Sect. 4, we shall show that the above-defined number n_{rect} plays an important role in the determination of the cardinalities of the sets of CC policies. For now, we note that, as shown in Fig. 5, the cardinality of the grid G is $|G| = \left(\sum_{i=1}^{n_{\text{rect}}} i\right) - 1 = \frac{n_{\text{rect}}(n_{\text{rect}}+1)}{2} - 1$, so it depends on n_{rect} only. We also mention that an application of [14, Lemma VII.6] provides sufficient conditions under which certain rows or columns of the grid G do not contain any corner point of an optimal CC policy (such conditions are extensions to nonlinearly constrained feasibility regions of analogous results obtained in [1]).

4 Narrowing the Search for Optimal CC Policies

The results described in Sect. 3 can be applied to narrow the search for optimal CC policies to those that satisfy the necessary optimality conditions stated in Propositions 3.2, 3.3, and 3.4. We call *candidate optimal CC policies* the CC policies that satisfy all or some of such conditions (the set of conditions actually considered in the characterization of a candidate optimal CC policy will be specified each time).

Table 1 Numbers of CC policies that satisfy the constraints coming from the necessary optimality conditions stated in Propositions 3.2, 3.3, and 3.4, for the feasibility region Ω_{FR} shown in Fig. 5.

Number of CC policies	
All policies	> 352715
Policies that satisfy Proposition 3.4	41
Policies that satisfy Propositions 3.3 and 3.4	28
Policies that satisfy Propositions 3.2, 3.3, and 3.4	15

As an example of application of the results that will be described later in this section, Table 1 shows how the number of candidate optimal CC policies for the feasibility region depicted in Fig. 5 decreases when each of the necessary optimality conditions above is added. We shall see that, when n_{rect} is "sufficiently small" our results can be exploited to find the optimal CC policies with a low computational burden (e.g., by exhaustive searches on various sets of candidate optimal CC policies). In general, we shall show that the cardinalities of the sets of candidate optimal CC policies are far smaller than both the cardinality of the set of all CC subsets of Ω_{FR} and the number $2^{|G|}$ of subsets of G.

In the following, we denote by $\mathscr{S}$ the set of all CC policies whose corner points are on the grid G, and by $|\mathscr{S}|$ its cardinality. By Proposition 3.1, any CC policy is completely identified by the set of its corner points, so $2^{|G|}$ is an upper bound on $|\mathscr{S}|$. However, not all subsets of points on the grid G are admissible as sets of corner points of a CC policy. Indeed, if one orders such corner points increasingly with respect to their first coordinates, then for any two successive corner points (α_i, β_i) and $(\alpha_{i+1}, \beta_{i+1})$, with $\alpha_i < \alpha_{i+1}$, the coordinate-convexity of the policy imposes the constraint

$$\beta_i > \beta_{i+1}. \tag{14}$$

This, combined with Proposition 3.4, implies that any optimal CC policy has at most $n_{rect} \leq \min\left\{n_{1,\max}^{\Omega_{FR}}, n_{2,\max}^{\Omega_{FR}}\right\}$ corner points. It also implies that, if a CC policy has a corner point (α, β), then it cannot have other corner points inside the rectangle of vertices $(0, 0)$, $(\alpha, 0)$, (α, β), and $(0, \beta)$. Concluding, if a CC policy has a corner point that belongs to G, then some other points of G cannot be corner points for that policy. Note also that, if the potential corner points are chosen in such a way that the previous constraints (14) are satisfied, then the set $\Omega_{FR} \setminus \cup_{i=1}^{|I(\Omega)|} C_i^-$ (see Proposition 3.1) is CC (this can be checked, e.g., by applying the characterization of coordinate-convexity provided by Proposition 2.1).

As shown by next Proposition 4.1, the number $|\mathscr{S}|$ of all CC policies whose corner points belong to the grid G depends only on the quantity n_{rect}. As they are CC, such policies satisfy the constraints (14). Moreover, Proposition 4.1 shows the exact dependence of $|\mathscr{S}|$ on n_{rect}. In order to make explicit such a dependence, we denote such a cardinality by $|\mathscr{S}(n_{rect})|$.

Proposition 4.1 *For $n_{rect} \geq 1$, one has $|\mathscr{S}(n_{rect})| = \frac{1}{n_{rect}+2}\binom{2(n_{rect}+1)}{n_{rect}+1} - 1 = C_{n_{rect}+1} - 1$, where, for a nonnegative integer n, C_n is the n-th Catalan number, defined as $C_n := \frac{1}{n+1}\binom{2n}{n}$.*

Fig. 6 An auxiliary feasibility region $\hat{\Omega}_{FR}$ with a grid $\hat{G}$ of the same form as the one associated with the feasibility region shown in Fig. 5

Fig. 7 A monotonic path associated with the CC subset $\{(0, 0), (0, 1), (0, 2), (1, 0), (1, 1), (1, 2), (2, 0), (3, 0)\}$ of the auxiliary feasibility region $\hat{\Omega}_{FR}$ shown in Fig. 6

Proof We note from Fig. 5 that the number of CC policies with corner points on the grid G of Ω_{FR} is equal to the number of CC policies with corner points on the grid $\hat{G}$ of the auxiliary feasibility region $\hat{\Omega}_{FR}$, shown in Fig. 6, which is characterized by the same value of n_{rect}. Indeed, the shape of the grid G depends only on n_{rect}. In particular, it does not depend on the coordinates of its points (which, instead, do depend on the feasibility region). Moreover, such a number is equal to the number of all CC subsets of $\hat{\Omega}_{FR}$.

Now, let us refer to Fig. 7. For $n = n_{\text{rect}} + 1$, the number of CC subsets of the auxiliary feasibility region $\hat{\Omega}_{FR}$ is equal to the number of different monotonic paths[4] along the edges of a grid with $n \times n$ square cells that do not lie above the NW-SE diagonal, excluding the monotonic path $(-1, n_{\text{rect}}) \to (-1, -1) \to (n_{\text{rect}}, -1)$, which does not correspond to any CC subset of $\hat{\Omega}_{FR}$. It is well known [20] that such a number of monotonic paths is the n-th Catalan number C_n minus 1, since the path $(-1, n_{\text{rect}}) \to (-1, -1) \to (n_{\text{rect}}, -1)$ has to be excluded from the enumeration. So, we get $|\mathcal{S}(n_{\text{rect}})| = C_{n_{\text{rect}}+1} - 1 = \frac{1}{n_{\text{rect}}+2}\binom{2(n_{\text{rect}}+1)}{n_{\text{rect}}+1} - 1$. □

As an example, for $n_{\text{rect}} = 1, 2, 3, 4$, Proposition 4.1 gives $|\mathcal{S}(n_{\text{rect}})| = 1, 4, 13, 41$, respectively. Interestingly, we shall see that $|\mathcal{S}(n_{\text{rect}})|$ can be computed also by Proposition 5.1 (see Sect. 5).

---

[4] Recall that a monotonic path (see also [20]) is a path that starts in the upper-left corner, finishes in the lower-right corner, and consists entirely of edges pointing rightward or downward.

Fig. 8 The sub-grid $\hat{G}'$ for the auxiliary feasibility region $\hat{\Omega}_{FR}$ shown in Fig. 6
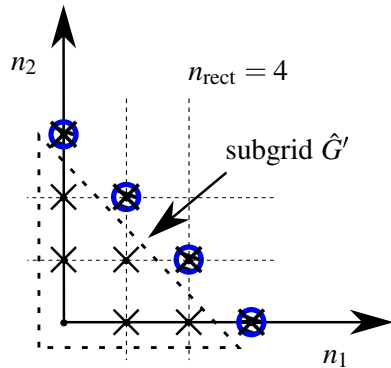
The number of candidate optimal CC policies can be further decreased by imposing the other structural properties of the optimal CC policies, described in Sect. 3. In particular, additional constraints on the locations of the corner points of an optimal CC policy follow from the general structural properties stated in Propositions 3.2 and 3.3.

In the following, we denote by $\mathscr{S}'(n_{\text{rect}})$ the set of all CC policies with corner points on the grid G (i.e., satisfying Proposition 3.4) that satisfy also Proposition 3.3. Next result provides the exact cardinality $|\mathscr{S}'(n_{\text{rect}})|$ of such a set.

Proposition 4.2 *For $n_{\text{rect}} = 1$, one has $|\mathscr{S}'(n_{\text{rect}})| = 1$. For $n_{\text{rect}} \geq 2$, one has*

$$
\begin{aligned}
|\mathscr{S}'(n_{\text{rect}})| &= |\mathscr{S}(n_{\text{rect}})| - |\mathscr{S}(n_{\text{rect}} - 1)| \\
&= C_{n_{\text{rect}}+1} - C_{n_{\text{rect}}} = \frac{1}{n_{\text{rect}} + 2}\binom{2(n_{\text{rect}} + 1)}{n_{\text{rect}} + 1} - \frac{1}{n_{\text{rect}} + 1}\binom{2(n_{\text{rect}})}{n_{\text{rect}}}.
\end{aligned}
\tag{15}
$$

Proof For $n_{\text{rect}} = 1$, the result follows directly by the fact that Ω_{FR} is rectangular, and the grid is empty. So, the set $\mathcal{S}(1)$ is made only of one policy, which is the *complete sharing policy* (i.e., the CC policy obtained for $\Omega = \Omega_{FR}$) that satisfies also Proposition 3.3.

For $n_{\text{rect}} \geq 2$, the proof is obtained by an application of Proposition 4.1. Indeed, by proceeding likewise in its proof, one can assume without any loss of generality that the feasibility region is $\hat{\Omega}_{FR}$ shown in Fig. 6. Now, for such an auxiliary feasibility region and $n_{\text{rect}} \geq 2$, the number of CC policies with corner points on the grid $\hat{G}$ and intersect its upper boundary is obtained by subtracting from the total number $C_{n_{\text{rect}}+1} - 1$ of CC policies, determined by Proposition 4.1, the number of CC policies with corner points on the sub-grid $\hat{G}'$ shown in Fig. 8. As $\hat{G}'$ takes on the same form as $\hat{G}$ (with n_{rect} replaced by $n_{\text{rect}} - 1$), such a number can be computed by Proposition 5.1, so it is equal to $C_{n_{\text{rect}}} - 1$. Hence, we get (15). □

As an example, for $n_{\text{rect}} = 1, 2, 3$, and 4 Proposition 4.2 gives $|\mathcal{S}'(n_{\text{rect}})| = 1, 3, 9$, and 28, respectively.

Fig. 9 The monotonic path
$(2, 1, 2)$ associated with the CC
subset
$\{(0, 0), (0, 1), (0, 2), (1, 0),$
$(1, 1), (1, 2), (2, 0), (2, 1)\}$ of
the auxiliary feasibility region
$\hat{\Omega}_{FR}$ shown in Fig. 6
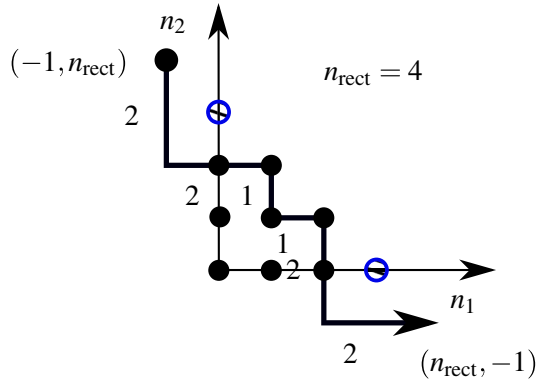
In the following, we denote by $\mathcal{S}''(n_{\text{rect}})$ the set of all CC policies with corner points on the grid G (i.e., that satisfy Proposition 3.4) that satisfy also Propositions 3.2 and 3.3. Next result provides the cardinality $|\mathcal{S}''(n_{\text{rect}})|$ of such a set.

Proposition 4.3 *For $n_{\text{rect}} \geq 1$, one has $|\mathcal{S}''(n_{\text{rect}})| = 2^{n_{\text{rect}}} - 1$.*

Proof Proceeding likewise in the proofs of Propositions 4.1 and 4.2, we refer to the feasibility region $\hat{\Omega}_{FR}$ shown in Fig. 6. Each CC policy with corner points on the grid $\hat{G}$ and satisfying Propositions 3.2 and 3.3 can be represented by a suitable monotonic path starting from the point $(-1, n_{\text{rect}})$ and ending in the point $(n_{\text{rect}}, -1)$ (see Fig. 9). The only additional requirements on such a monotonic path are the following:

1. It is not the monotonic path $(-1, n_{\text{rect}}) \rightarrow (-1, -1) \rightarrow (n_{\text{rect}}, -1)$, which is associated to no CC policy;
2. Each time a number of consecutive unit steps downward is made, the same number of consecutive unit steps is made rightward as the path changes its direction.

From Figure 9 one can see that the two constraints are equivalent to requiring that the monotonic path intersects $(\partial \Omega_{FR})^+$ and that the associated CC policy satisfies Proposition 3.2.

Moreover, the particular form of this monotonic path implies that the path itself can be represented merely by its ordered sequence of steps downward, e.g., $(2, 1, 2)$ in Fig. 9. In general, each such path can be represented by a sequence $(l_1, \ldots, l_h)$, where $l_1, \ldots, l_h$ are $h \leq n_{\text{rect}} + 1$ positive integers and $\sum_{i=1}^{h} l_i = n_{\text{rect}} + 1$ (the unique sequence to be excluded is the one with $h = 1$ and $l_1 = n_{\text{rect}} + 1$, which corresponds to the monotonic path $(-1, n_{\text{rect}}) \rightarrow (-1, -1) \rightarrow (n_{\text{rect}}, -1)$). Now, recall that, for each positive integer n, the number $P(n)$ of distinct ordered sequences $(l_1, \ldots, l_h)$ with $h \leq n$ such that $\sum_{i=1}^{h} l_i = n$ is equal to 2^{n-1}. Indeed, a simple dynamic-programming argument shows that, setting $P(0) := 1$, one has $P(n) = \sum_{k=1}^{n} P(n-k)$ for $n \geq 1$, from which one concludes by induction that $P(n) = 2^{n-1}$ for $n \geq 1$.

Summing up, the number of CC policies with corner points on the grid $\hat{G}$ and satisfying Propositions 3.2 and 3.3 is equal to $2^{n_{\text{rect}}} - 1$. $\square$

Fig. 10 The path associated with the CC subset $\{(0,0),(0,1),(0,2),(0,3),(1,0),(1,1),(1,2),(1,3),(2,0),(2,1),(2,2),(3,0),(4,0)\}$ of the rectangular feasibility region $\Omega_{FR} = H_R = \{0,1,\ldots,5\} \times \{0,1,\ldots,4\}$
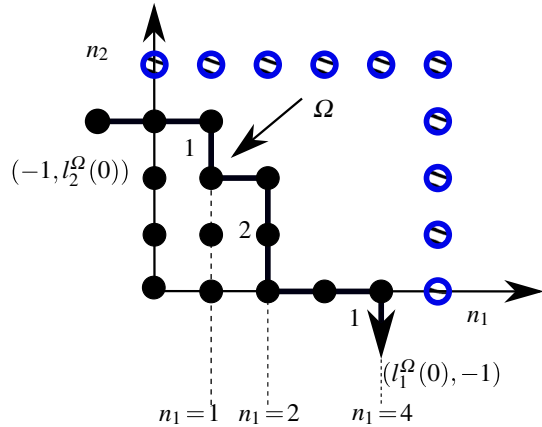
As an example, for $n_{\text{rect}} = 1, 2, 3, 4$ Proposition 4.3 gives $|\mathscr{S}''(n_{\text{rect}})| = 1, 3, 7, 15$, respectively. Of course, in general $|\mathscr{S}(n_{\text{rect}})| \geq |\mathscr{S}'(n_{\text{rect}})| \geq |\mathscr{S}''(n_{\text{rect}})|$, and for $n_{\text{rect}} = 1$ one has $|\mathscr{S}(1)| = |\mathscr{S}'(1)| = |\mathscr{S}''(1)| = 1$.

It is interesting to compare the expressions of $|\mathcal{S}(n_{\text{rect}})|$, $|\mathcal{S}'(n_{\text{rect}})|$, and $|\mathcal{S}''(n_{\text{rect}})|$ given in Propositions 4.1, 4.2 and 4.3, respectively, with the cardinality $|\mathcal{S}_{CC}(\Omega_{FR})|$ of the set $\mathcal{S}_{CC}(\Omega_{FR})$ of all CC subsets of Ω_{FR}, without imposing the constraints coming from Propositions 3.2, 3.3, and 3.4. Note that such a cardinality does not depend on n_{rect}, in the sense that different feasibility regions Ω_{FR} with the same n_{rect} may have different values of $|\mathcal{S}_{CC}(\Omega_{FR})|$. Let us start by considering the case of a particularly simple feasibility region, i.e., a rectangular one, which we denote by H_R.

Proposition 4.4 *For a rectangular feasibility region H_R, one has*

$$|\mathcal{S}_{CC}(H_R)| = \frac{\left(n_{1,\max}^{H_R} + n_{2,\max}^{H_R} + 2\right)!}{\left(n_{1,\max}^{H_R} + 1\right)!(n_{2,\max}^{H_R} + 1)!} - 1.$$

Proof For a rectangular feasibility region H_R, each CC set $\Omega \subseteq H_R$ can be represented by a path made only of steps rightward and downward, starting rightward from the point $\left(-1, l_2^{\Omega}(0)\right)$ and ending downward in the point $\left(l_1^{\Omega}(0), -1\right)$ (see Fig. 10 for an example). Such a path has a total number of $l_2^{\Omega}(0) + 1$ steps downward at locations taken from the set $\left\{0, \ldots, n_{1,\max}^{H_R}\right\}$, where the same location can figure more than once (for instance, the path represented in Fig. 10 has 1 step downward for $n_1 = 1$, 2 steps for $n_1 = 2$, and 1 step for $n_1 = 4$). So, each CC set $\Omega \subseteq H_R$ with a given $l_2^{\Omega}(0)$ can be associated in a one-to-one way to a combination with repetition of k elements from $\left\{0, \ldots, n_{1,\max}^{H_R}\right\}$ of cardinality $n = n_{1,\max}^{H_R} + 1$, where $k = l_2^{\Omega}(0) + 1 \in \left\{1, \ldots, n_{2,\max}^{H_R} + 1\right\}$. The number of such different combinations is denoted by $\left(\!\!\binom{n}{k}\!\!\right)$, which is equal to $\binom{n+k-1}{k} = \frac{(n+k-1)!}{k!(n-1)!}$ (see, e.g., [21, p. 16]). Summing over all

possible values of $l_2^\Omega(0) \in \left\{0, \ldots, n_{2,\max}^{H_R}\right\}$, we get $|\mathcal{S}_{CC}(H_R)| = \sum_{k=1}^{n_{2,\max}^{H_R}+1} \binom{n_{1,\max}^{H_R}+1}{k}$.
Then, by exploiting the equality $\sum_{k=1}^{h} \binom{m}{k} = \binom{n+1}{h} - 1$ from [21, p. 16], we get
$$|\mathcal{S}_{CC}(H_R)| = \binom{n_{1,\max}^{H_R}+2}{n_{2,\max}^{H_R}+1} - 1 = \frac{\left(n_{1,\max}^{H_R}+n_{2,\max}^{H_R}+2\right)!}{\left(n_{1,\max}^{H_R}+1\right)!\left(n_{2,\max}^{H_R}+1\right)!} - 1. \qquad \square$$

As an example, for $n_{1,\max} = 4$ and $n_{2,\max} = 5$ Proposition 4.4 gives $|\mathcal{S}_{CC}(H_R)| = 425$. It follows also from the definitions that, for a rectangular feasibility region (for which $n_{\text{rect}} = 1$), one has $|\mathcal{S}_{CC}(H_R)| \geq |\mathcal{S}(1)| = 1$, and in general, for $n_{1,\max}^{H_R}$ and $n_{2,\max}^{H_R}$ "not too small", $|\mathcal{S}_{CC}(H_R)| \gg |\mathcal{S}(1)| = 1$. Similarly, for a rectangular feasibility region H_R contained in a nonrectangular one Ω_{FR}, one has obviously $|\mathcal{S}_{CC}(H_R)| \leq |\mathcal{S}_{CC}(\Omega_{FR})|$, and when $\min\{n_{1,\max}^{H_R}, n_{2,\max}^{H_R}\}$ is "not too small" with respect to the value of n_{rect} associated with Ω_{FR}, Propositions 4.1 and 4.4 imply $|\mathcal{S}_{CC}(H_R)| \gg |\mathcal{S}(n_{\text{rect}})|$. This is the way we estimated the lower bound 352715 on the number of all CC policies in the example in Table 1, for which we applied Proposition 4.4 to the rectangular subregion $\{0, 1, \ldots, 9\} \times \{0, 1, \ldots, 10\}$ of the feasibility region Ω_{FR} shown in Fig. 5.

We conclude this section by mentioning that a way to compute $|\mathcal{S}_{CC}(\Omega_{FR})|$ exactly for the general case of a nonlinearly constrained feasibility region is provided by Remark 5.1 in Sect. 5.

5 A Graph-Based Algorithm to Generate All Candidate Optimal CC Policies

In this section, we describe a graph-based algorithm to generate all candidate optimal CC policies for $n_{\text{rect}} > 1$ (the case $n_{\text{rect}} = 1$ is trivial, as it is associated with a rectangular feasibility region and an empty grid). Moreover, in Proposition 5.1 we provide a variation of Proposition 4.1, which allows one to compute in a different way the number $|\mathcal{S}|$ of all CC policies with all their corner points on the grid G.

We start the analysis by showing how one can associate in a one-to-one way each CC policy having all corner points on the grid G, with a directed path in a suitable auxiliary *directed acyclic graph* (*DAG*). Figure 11 shows that how this auxiliary graph is constructed for the case of the feasibility region Ω_{FR} in Fig. 5.

First of all, we build the auxiliary feasibility region $\hat{\Omega}_{FR}$ in Fig. 6, which is characterized by the same value of n_{rect} as Ω_{FR} (in this case, $n_{\text{rect}} = 3$). As such, its grid $\hat{G}$ has the same shape as the one associated with Ω_{FR}, and the CC policies with all their corner points on the grid G of Ω_{FR} are associated in a one-to-one way with the CC policies whose corner points belong to the grid $\hat{G}$ of $\hat{\Omega}_{FR}$.

Then, we construct an auxiliary graph, whose vertices are divided into layers. For $j = 1, \ldots, n_{\text{rect}}$, the j-th layer contains all the points in the grid $\hat{G}$, whose first coordinate n_1 is equal to $n_{1,\max}^{\hat{\Omega}_{FR}} - j + 1$ (for instance, in Fig. 11 the first layer contains only the vertex $(3, 0)$). The last layer $n_{\text{rect}} + 1$ contains the auxiliary vertices $(0, 1)^+, \ldots, (0, n_{\text{rect}} - 1)^+$ and a vertex labeled as "$-$" (to distinguish the vertices of the last layer, we represent them by dashed circles). There are two kinds of arcs in the auxiliary graph: solid arcs and dashed arcs. For $j = 1, \ldots, n_{\text{rect}} - 1$, each vertex of coordinates (l_j, m_j) in the layer j is connected by solid arcs to all the vertices
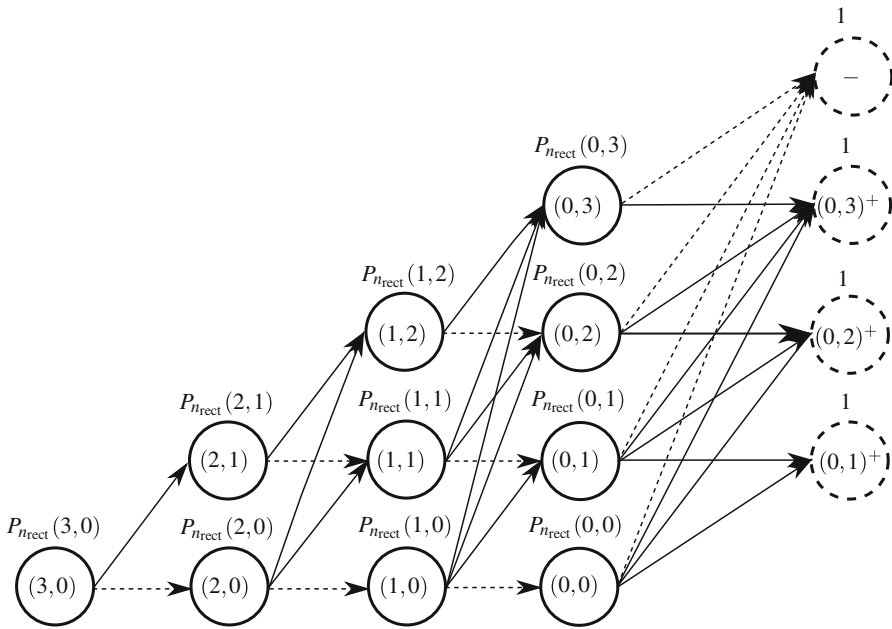
Fig. 11 The auxiliary graph associated with the auxiliary feasibility region $\hat{\Omega}_{FR}$ shown in Fig. 6

of the successive layer, whose second coordinate is greater than m_j. Moreover, it is also connected by a dashed arc to the unique vertex of the successive layer, whose second coordinate is equal to m_j. For $j = n_{\text{rect}}$, each vertex (l_j, m_j) in the layer j is connected by solid arcs to the vertices $(0, 1)^+, \ldots, (0, n_{\text{rect}} - 1)^+$ of the final layer, whose second coordinate is greater than or equal to m_j, and is connected by a dashed arc to the auxiliary vertex "$-$."

Now, we consider in the auxiliary graph a directed path that starts from the only vertex in the first layer and ends into any one of the vertices in the final layer. As we move from one layer to next one, we build the CC policy associated with the directed path by updating the list of its corner points (initialized by an empty list at the starting vertex). Suppose that, when moving along the directed path, we are currently at the vertex (l_j, m_j) in layer j ($j = 1, \ldots, n_{\text{rect}}$). If a dashed transition is made to a vertex in a successive layer, then no corner point is added to the list. Instead, if $j = 1, \ldots, n_{\text{rect}} - 1$ and a solid transition is made to the vertex (l_{j+1}, m_{j+1}), then the point $(l_{j+1} + 1, m_{j+1} - 1)$ is added to the list of corner points. Finally, if $j = n_{\text{rect}}$ and a solid transition is made to the vertex $(l_{j+1}, m_{j+1})^+$, then the corner point (l_{j+1}, m_{j+1}) is added to the list. For instance, the corner points of the CC policy associated with the directed path $(3, 0) \rightarrow (2, 1) \rightarrow (1, 1) \rightarrow (0, 3) \rightarrow$ "$-$" in Fig. 11 are $(3, 0)$ and $(1, 2)$. The CC policy associated with the directed path $(3, 0) \rightarrow (2, 0) \rightarrow (0, 0) \rightarrow (0, 1) \rightarrow$ "$-$" in Fig. 11 has no corner points and is the complete sharing policy.

It follows by the construction of the auxiliary graph (basically, from the absence of NW-SE transitions) that, each time a corner point is added to the current list of

corner points, the constraints (14) are satisfied for all the current corner points in the list. Moreover, all the CC policies of $\hat{\Omega}_{FR}$ can be constructed in the way described above, and no two different directed paths can be associated with the same CC policy. Of course, once all the CC policies for $\hat{\Omega}_{FR}$ have been generated by an enumeration of the corresponding directed paths, one can generate the ones with corner points on the grid G of the original feasibility region Ω_{FR}, by identifying the points of the grid $\hat{G}$ with the corresponding ones of the grid G, which has the same shape as $\hat{G}$.

Summing up, the number of different CC policies of $\hat{\Omega}_{FR}$ (which is equal to $|\mathcal{S}(n_{\text{rect}})|$) corresponds to the number of different directed paths going from the unique vertex in the first layer into any one of the vertices in the final layer. This number can be computed by a dynamic-programming argument, as shown in the following proposition. The case $n_{\text{rect}} = 1$, which is not included in Proposition 5.1, is trivial and gives $|\mathcal{S}(1)| = 1$.

Proposition 5.1 *Let* $n_{\text{rect}} > 1$. *Then* $|\mathcal{S}(n_{\text{rect}})| = P_{n_{\text{rect}}}(n_{\text{rect}} - 1, 0)$, *where* $P_{n_{\text{rect}}}(n_{\text{rect}} - 1, 0)$ *is computed recursively as follows:*

$$P_{n_{\text{rect}}}(0, 0) := n_{\text{rect}}, \tag{16}$$

$$P_{n_{\text{rect}}}(0, j) := n_{\text{rect}} + 1 - j, \quad j = 1, \ldots, n_{\text{rect}} - 1, \tag{17}$$

$$P_{n_{\text{rect}}}(i, j) := \sum_{k=j}^{n_{\text{rect}}-i} P_{n_{\text{rect}}}(i - 1, k), \quad i = 1, \ldots, n_{\text{rect}} - 1, \quad j = 0, \ldots, n_{\text{rect}} - i - 1. \tag{18}$$

Proof By the discussion in Sect. 5, $|\mathcal{S}(n_{\text{rect}})|$ is equal to the number of different directed paths originating from the unique vertex in the first layer and ending into any one of the vertices in the final layer of the auxiliary graph shown in Fig. 11. We denote by $P_{n_{\text{rect}}}(i, j)$ the number of different directed sub-paths starting from the vertex (i, j) in the auxiliary graph, when the vertex appears in any layer with the exception of the last one (for the vertices in the last layer there is only one directed sub-path). Inspection of Fig. 11 shows that formulas (16) and (17) hold for the second last layer. Moreover, due to the structure of the auxiliary graph, the number of directed sub-paths starting from a vertex in one of the first layers is equal to the sum of all the directed sub-paths starting from its neighbors in the successive layer, so it is given by (18). □

Interestingly, one has the following alternative interpretation of the quantities $P_{n_{\text{rect}}}(i, j)$ in Proposition 5.1 and the following alternative proof.

For each point (i, j) of $\hat{\Omega}_{FR}$ with $j = 0$, let $P_{n_{\text{rect}}}(i, j)$ be the number of CC sets $\hat{\Omega}'$ that satisfy the condition $\hat{\Omega}' \subseteq \{(n_1, n_2) \in \hat{\Omega}_{FR} : n_1 \leq i\}$. Similarly, for each point (i, j) of $\hat{\Omega}_{FR}$ with $j > 0$, let $P_{n_{\text{rect}}}(i, j)$ be the number of CC sets $\hat{\Omega}''$ such that $(i, j - 1) \in \hat{\Omega}''$ and $\hat{\Omega}'' \subseteq \{(n_1, n_2) \in \hat{\Omega}_{FR} : n_1 \leq i\}$. Then $|\mathcal{S}(n_{\text{rect}})| = P_{n_{\text{rect}}}(n_{\text{rect}} - 1, 0)$ and formulas (16) and (17) follow directly from the previous two definitions of $P_{n_{\text{rect}}}(i, j)$ for $i = 0$.

We compute $P_{n_{\text{rect}}}(n_{\text{rect}} - 1, 0)$ recursively, showing that (18) holds. Let (i, j) be a point of $\hat{\Omega}_{FR}$ with $i > 0$, $P_{n_{\text{rect}}}^+(i, j)$ the number of CC sets $\hat{\Omega}'''$ such that (i, j) is a

corner point of $\hat{\Omega}'''$, and $\hat{\Omega}''' \subseteq \{(n_1, n_2) \in \hat{\Omega}_{FR} : n_1 \leq i\}$. Then, by the definitions of $P_{n_{\text{rect}}}$ and $P_{n_{\text{rect}}}^+$, we get $P_{n_{\text{rect}}}^+(i, j) = P_{n_{\text{rect}}}(i - 1, j + 1)$ and

$$
P_{n_{\text{rect}}}(i, j) = \sum_{k=j}^{n_{\text{rect}}-i-1} P_{n_{\text{rect}}}^+(i, k) + P_{n_{\text{rect}}}(i - 1, j) = \sum_{k=j}^{n_{\text{rect}}-i-1}
$$

$$
\times P_{n_{\text{rect}}}(i - 1, k + 1) + P_{n_{\text{rect}}}(i - 1, j) = \sum_{k=j}^{n_{\text{rect}}-i} P_{n_{\text{rect}}}(i - 1, k),
$$

which complete the proof of (18).

As an example, for $n_{\text{rect}} = 4$, Proposition 5.1 provides

- $P_{n_{\text{rect}}}(0, 0) = 4, P_{n_{\text{rect}}}(0, 1) = 4, P_{n_{\text{rect}}}(0, 2) = 3, P_{n_{\text{rect}}}(0, 3) = 2$;
- $P_{n_{\text{rect}}}(1, 0) = 4 + 4 + 3 + 2 = 13, P_{n_{\text{rect}}}(1, 1) = 4 + 3 + 2 = 9, P_{n_{\text{rect}}}(1, 2) = 3 + 2 = 5$;
- $P_{n_{\text{rect}}}(2, 0) = 13 + 9 + 5 = 27, P_{n_{\text{rect}}}(2, 1) = 9 + 5 = 14$;
- $P_{n_{\text{rect}}}(3, 0) = 27 + 14 = 41$.

So, $|\mathscr{S}(4)| = P_{n_{\text{rect}}}(3, 0) = 41$ (of course, this is the same estimate provided by Proposition 4.1).

Remark 5.1 Compared with Proposition 4.1, Proposition 5.1 provides a less compact representation of $|\mathscr{S}(n_{\text{rect}})|$. However, the technique of the auxiliary graph used to prove Proposition 5.1 can be exploited to prove suitable variations of Proposition 5.1, aimed at computing the following quantities.

1. The number $|\mathscr{S}_{CC}(\Omega_{FR})|$ of all CC subsets of the feasibility region Ω_{FR}. This can be obtained by constructing an auxiliary graph similar to the one in Fig. 11, and counting the number of all directed paths from the first layer to the last one. The auxiliary graph is constructed in such a way that the layer j has $l_2^{\Omega_{FR}}(j - n_{1,\max} - 1)$ vertices, for $j = 1, \ldots, n_{1,\max}^{\Omega_{FR}} + 1$, and $l_2^{\Omega_{FR}}(0)$ vertices, for $j = n_{1,\max}^{\Omega_{FR}} + 2$.
2. The number of all CC subsets of Ω_{FR} with all corner points on the grid G, but not belonging to certain rows or columns of G on which it is known a-priori that an optimal CC policy has no corner points (e.g., by an application of [14, Lemma VII.6]). This number can be computed by removing the corresponding rows or columns of points in the auxiliary feasibility region $\hat{\Omega}_{FR}$ (thus, "squeezing" $\hat{\Omega}_{FR}$), and proceeding likewise in item 1. □

Once all the CC policies with corner points on the grid $\hat{G}$ have been generated in the above-described graph-based algorithm, one can remove from such a set all the CC policies that do not satisfy Proposition 3.3. It follows from the proof of Proposition 4.2 that the latter policies can be obtained by the same algorithm, applied to a smaller feasibility region, which differs from $\hat{\Omega}_{FR}$ by the translation of $(\partial\hat{\Omega}_{FR})^+$ one step downward. Finally, among the remaining policies, those that do not satisfy Proposition 3.2 can be simply obtained by looking at all the policies with at least two corner points, and removing from the current list of candidate optimal policies all those for which the point $(\alpha_{i+1} - 1, \beta_i - 1)$ is strictly inside $\hat{\Omega}_{FR}$ for at

Table 2 Corner points of the CC policies generated by the algorithm described in Sect. 5, for the auxiliary feasibility region $\hat{\Omega}_{FR}$ shown in Fig. 6.

CC policies that satisfy Proposition 3.4, but not Propositions 3.2 and 3.3

(3, 0), (2, 1), (1, 2), (0, 3)

(3, 0), (2, 1), (0, 2)

(3, 0), (1, 1), (0, 2)

(3, 0), (1, 1), (0, 3)

(3, 0), (0, 1)

(2, 0), (1, 2), (0, 3)

(2, 0), (1, 1), (0, 2)

(2, 0), (1, 1), (0, 3)

(2, 0), (0, 1)

(2, 0), (0, 2)

(1, 0), (0, 1)

(1, 0), (0, 2)

(1, 0), (0, 3)

CC policies that satisfy Propositions 3.3 and 3.4, but not Proposition 3.2

(3, 0), (2, 1), (1, 2)

(3, 0), (2, 1)

(3, 0), (2, 1), (0, 3)

(3, 0), (1, 2), (0, 3)

(3, 0), (1, 1)

(2, 1), (1, 2)

(2, 1), (1, 2), (0, 3)

(2, 1), (0, 2)

(2, 0), (1, 2)

(2, 0), (1, 1)

(1, 2), (0, 3)

(1, 1), (0, 2)

(1, 1), (0, 3)

CC policies that satisfy Propositions 3.2, 3.3, and 3.4

(3, 0), (1, 2)

(3, 0)

(3, 0), (0, 2)

(3, 0), (0, 3)

(2, 1)

(2, 1), (0, 3)

(2, 0)

(2, 0), (0, 3)

(1, 2)

(1, 1)

(1, 0)

Table 2 continued

no corner points
(0, 1)
(0, 2)
(0, 3)

Table 3 Association between the points of the grid $\hat{G}$ of $\hat{\Omega}_{FR}$ and those of the grid G of Ω_{FR}, for the example, shown in Fig. 5.

Grid	$\hat{G}$	(1,0)	(2,0)	(3,0)	(0,1)	(1,1)	(2,1)	(0,2)	(1,2)	(0,3)
	G	(5,0)	(10,0)	(12,0)	(0,4)	(5,4)	(10,4)	(0,8)	(5,8)	(0,11)

least one pair of consecutive corner points (α_i, β_i) and $(\alpha_{i+1}, \beta_{i+1})$. After these last removals, one obtains all the CC policies with corner points on the grid $\hat{G}$ that satisfy Propositions 3.2 and 3.3 (alternatively, one can generate such policies directly in a recursive way, using the dynamic-programming argument of the proof of Proposition 4.3).

Table 2 shows all the CC policies generated by the algorithm described in this section for the auxiliary feasibility region $\hat{\Omega}_{FR}$ shown in Fig. 6. For each policy, only the list of its corner points is shown in the table. Finally, Table 3 shows the association between the points of the grid $\hat{G}$ of $\hat{\Omega}_{FR}$ and those of the grid G of Ω_{FR}, for the example considered in Fig. 5.

6 Conclusions

For a generalized stochastic knapsack problem modeling call admission control (CAC) with two classes of users, we have provided an exact enumeration of all the coordinate-convex (CC) policies that satisfy certain optimality conditions. We have described a graph-based algorithm to generate all such policies. The results can be exploited to establish for which feasibility regions such optimality conditions restrict significantly the cardinalities of the sets of candidate optimal CC policies, with respect to the set of all CC subsets of Ω_{FR}.

Another possibility consists in replacing the feasibility region Ω_{FR} with feasibility regions $\Omega'_{FR} \subset \Omega_{FR}$ and $\Omega''_{FR} \supset \Omega_{FR}$ with "simpler" boundaries (in the sense that the associated values of n_{rect} are "significantly smaller" than the one associated with Ω_{FR}). Then, one evaluates the performances of all the CC policies generated by our graph-based algorithm applied to Ω'_{FR} and Ω''_{FR} instead of Ω_{FR}. In this way one obtains, respectively, a lower bound and an upper bound on the performance of an optimal CC policy for the original problem associated with Ω_{FR}. Moreover, greedy algorithms, like the one developed in [12], can be used to find sufficiently good suboptimal CAC policies which satisfy the previously mentioned necessary optimality conditions.

We conclude by mentioning that most structural results stated in Sect. 3 can be extended to more than two classes of users, which were considered in [14]. However,

it seems unlikely that in such a situation one can determine the cardinalities of various sets of candidate optimal policies by means of simple expressions like those obtained in Sect. 4 for two classes (an exception is when it is known a-priori that the optimal CC policies take on particularly simple forms (see, e.g., [14, Theorem IV.8 and Proposition VI.3])).

References

1. Ross, K., Tsang, D.: The stochastic knapsack problem. IEEE Trans. Commun. **37**(7), 740–747 (1989)
2. Kleywegt, A.J., Papastavrou, J.D.: The dynamic and stochastic knapsack problem with random sized items. Oper. Res. **49**(1), 26–41 (2001)
3. Dean, B.C., Goemans, M.X., Vondrak, J.: Approximating the stochastic knapsack problem: the benefit of adaptivity. Math. Oper. Res. **33**(4), 945–964 (2008)
4. Keller, H., Pferschy, U., Pisinger, D.: Knapsack Problems. Springer, Berlin Heidelberg (2004)
5. Kesidis, G., Walrand, J., Chang, C.S.: Effective bandwidths for multiclass Markov fluids and other ATM sources. IEEE ACM Trans. Netw. **1**(4), 424–428 (1993)
6. Ross, K.W.: Multiservice Loss Models for Broadband Telecommunication Networks. Springer, New York (1995)
7. Aswakul, C., Barria, J.: Analysis of dynamic service separation with trunk reservation policy. IEE Proc. Commun. **149**(1), 23–28 (2002)
8. Guerin, R., Ahmadi, H., Naghshineh, M.: Equivalent capacity and its application to bandwidth allocation in high-speed networks. IEEE J. Sel. Areas Commun. **9**(7), 968–981 (1991)
9. Tse, D., Gallager, R., Tsitsiklis, J.: Statistical multiplexing of multiple time-scale Markov streams. IEEE J. Sel. Areas Commun. **13**(6), 1028–1038 (1995)
10. Javidi, T., Teneketzis, D.: An approach to connection admission control in single-hop multiservice wireless networks with QoS requirements. IEEE Trans. Veh. Technol. **52**(4), 1110–1124 (2003)
11. Cello, M., Gnecco, G., Marchese, M., Sanguineti, M.: Structural properties of optimal coordinate-convex policies for CAC with nonlinearly-constrained feasibility regions. In: Proceedings of IEEE INFOCOM'11 Mini-Conf., pp. 466–470 (2011)
12. Cello, M., Gnecco, G., Marchese, M., Sanguineti, M.: CAC with nonlinearly-constrained feasibility regions. IEEE Commun. Lett. **15**(4), 467–469 (2011)
13. Dasylva, A., Srikant, R.: Bounds on the performance of admission control and routing policies for general topology networks with multiple call classes. In: Proceedings of IEEE INFOCOM'99, vol. 2, pp. 505–512 (1999)
14. Cello, M., Gnecco, G., Marchese, M., Sanguineti, M.: Optimality conditions for coordinate-convex policies in CAC with nonlinearly feasibility boundaries. IEEE ACM Trans. Netw. **21**(5), 1363–1377 (2013)
15. Hörmander, L.: Notions of Convexity. Birkäuser, Boston (2007)
16. Likhanov, N., Mazumdar, R.R., Theberge, F.: Providing QoS in large networks: Statistical multiplexing and admission control. In: Boukas, E., Malhame, R. (eds.) Analysis, Control and Optimization of Complex Dynamic Systems, pp. 137–167. Kluwer (2005)
17. Barnhart, C., Wieselthier, J., Ephremides, A.: An approach to voice admission control in multihop wireless networks. In: Proceedings of IEEE INFOCOM'93, vol. 1, pp. 246–255 (1993)
18. Bolla, R., Davoli, F., Marchese, M.: Bandwidth allocation and admission control in ATM networks with service separation. IEEE Commun. Mag. **35**(5), 130–137 (1997)
19. Little, J.D.C.: A proof for the queuing formula: $l = \lambda w$. Oper. Res. **9**(3), 383–387 (1961)
20. Stanley, R.P.: Enumerative Combinatorics, vol. 2. Cambridge University Press, Cambridge (1999)
21. Comtet, L.: Advanced Combinatorics: the Art of Finite and Infinite Expansions. Kluwer, Amsterdam (1974)